Journal of Theoretical and Applied Vibration and Acoustics 10 (2) 65-76 (2024)

I S A V

Journal of Theoretical and Applied Vibration and Acoustics

journal homepage: http://tava.isav.ir

Acoustic energy harvesting from sonic crystals with non-square lattices using piezoelectric patch

Saeed Sharifi Moghaddam*, **Saeed Ziaei-Rad**, **Reihaneh Hadipour Hafshjani**, **Reza Tikani**

Department of Mechanical Engineering, Isfahan University of Technology, Isfahan, IRAN

Research Article

ARTICLE INFO

Article history:
Received 28 February 2024

Received in revised form
13 February 2025

Accepted 22 February 2025

Available online 18 April 2025

Keywords:
Energy harvesting

Sonic crystal

Piezoelectric

Metamaterial

ABSTRACT

The field of energy harvesting from the environment has emerged as a significant area of research in recent years. Acoustic energy represents a natural source of mechanical energy that can be converted into electrical energy using metamaterials and piezoelectric materials. A defect was introduced into a regular lattice of the crystal. At the point of defect, a concentration of sound pressure was created, and by installing the PVDF piezoelectric patch, mechanical energy can be converted into electrical energy. In this study, an effort was made to identify a suitable model for maximum acoustic energy harvesting. The effect of various lattices, including circular, rhombus, rectangular, square-rhombic, square-rectangular, and rhombus-rectangular lattices, on the sound pressure level (SPL) and energy harvesting was investigated. Additionally, the impact of modifying the position of the defect and increasing the number of defects on the SPL was examined. The simulation results were calculated using COMSOL Multiphysics 6.0. The results were validated by comparing them with those of previous studies. Findings demonstrated that a square-rhombic lattice can provide the highest SPL and, consequently, the highest harvested energy. In the square-rhombic lattice, using the optimal resistance of 15 kΩ at the frequency of 4220.4 Hz yielded a voltage and power of 11.34 mV and 4.15 nW, respectively.

* Corresponding author.
E-mail address: saeid.sharifi@me.iut.ac.ir (S. Sharifi Moghadam)

http://dx.doi.org/10.22064/tava.2025.2023906.1233

1. Introduction

Energy harvesting has been an increasingly interesting topic for researchers in recent years, as it converts the waste energy of the environment into usable energy. Acoustic energy is considered one of the sources of energy that can be taken from the environment for reasons such as cleanliness and high accessibility [1-5]. A huge part of the energy in acoustic waves is lost during propagation. Typically, the energy density of acoustic waves is too low to be converted into other forms of energy. Therefore, researchers have proposed different ways to increase the energy density of acoustic waves. Materials with piezoelectric properties are widely used to convert mechanical (vibrational) energy into electrical energy [6-10]. Application of acoustic energy harvesting is used on noisy roads and streets and setting up wireless sensors [11]. One way to focus on acoustic energy is to use sonic crystals. Sonic crystals are materials that have different acoustic properties [7]. The concentration of pressure in the resonance frequency in sonic crystals increases the acoustic energy. A defect is created by removing a rod from regular sonic crystals and can act as a resonance cavity. If the piezoelectric is placed inside an acoustic crystal defect, the conversion of acoustic energy to electrical energy occurs at the resonance frequency of the cavity [12-14] .

Most previous research on energy harvesting has focused on the 2D periodic square lattice sonic crystal, consisting of circular rods immersed in a fluid. In this context, Wu et al. [15] presented acoustic energy harvesting using a sonic crystal. By removing the middle crystal, they arranged the cylindrical acoustic crystals in a 5×5 lattice. They found that the energy could be harvested when the acoustic frequency generated in the defect matched the resonance frequency of the sonic crystal. By placing a PVDF piezoelectric film at the defect's location, they obtained a maximum power of 35 nW from acoustic waves at a pressure of about 80 to 100 dB and a frequency of 4.2 kHz with a resistance of 9.3 kΩ. In the same year, Wu et al. [16] compared a 5×5 lattice with 7×6 and 9×7 lattices numerically and experimentally. They demonstrated that the resonance frequencies in all three lattices are very close to one another. They also found that as the number of cylinders behind the defect increases, the sound becomes more concentrated, with higher pressure. Consequently, at a frequency of 5.15 kHz, the sound pressure in lattices of 5×5, 6×7, and 7×9 equals 6.79 Pa, 23.42 Pa, and 27.073 Pa, respectively. Carrera et al. [17] presented a phononic crystal model featuring a semi-elliptical lattice attached to a flat plate to enhance electrical energy harvesting. Their research showed that the frequency range of energy harvesting was 30-70 kHz, and the maximum absorbed power was nearly 40 times larger than the case without a lattice. Yang et al. [1] used a Helmholtz resonator in the crystal cavity to increase the acoustic energy density, thereby increasing energy harvesting. They showed that acoustic energy harvesting, in this case, is 23 times greater than sonic crystals with a defect alone and 262 times greater than that of the Helmholtz resonator alone. They obtained a power of 429 μW at a frequency of 5.545 kHz with a resistance equal to 4.4 kΩ.

In this study, for the first time, the acoustic behavior of 2D periodic non-square lattice sonic crystals is investigated and compared to identify a suitable model of the crystal lattice to increase the SPL and harvest the maximum energy. Non-square lattices have been studied, including circular, rhombus-shaped, rectangular, square-rhombic, square-rectangular, and rhombus-rectangular lattices. Also, the effect of changing the position of the defect and the number of defects on the SPL value in the square lattice of crystals has been investigated. This model is simulated by using the Comsol Multiphysics 6.0 software. The obtained results from different lattices are compared.

In the second part of the paper, the modeling method of the problem is presented. The third part presents the simulation results obtained using the Comsol software, followed by the conclusion.

2. Simulation of the sonic crystals

In the current model, the crystals are made of polymethyl methacrylate(PMMA), and sound is propagated in air. The sound propagation environment is considered a spherical space with a radius of 60 cm around the crystals. The radius of the cylinders (r_0) is 17.5 mm, and their center-to-center distance (a_0) is 49 mm. Additionally, a disk with a diameter of 140 mm and a thickness of 17.5 mm is considered to produce sound with a pressure of 1Pa.

The position of the sound source relative to the crystals is shown in Figure 1. A piezoelectric beam with dimensions of 63×16×0.028 mm^3 is chosen because its natural frequency is close to the acoustic resonance frequency. In this study, a static-acoustic-piezoelectric multi-physics module is used in COMSOL Multiphysics 6.0 software. To harvest energy, a piezoelectric material with a PVDF model has been used because this type of piezoelectric material is soft and vibrates more under small excitation. PVDF is installed at the position of the defect, where the maximum pressure difference occurs. The number of elements considered for this model after convergence is equal to 374293. The properties related to PMMA and piezoelectric materials are presented in Table 1.

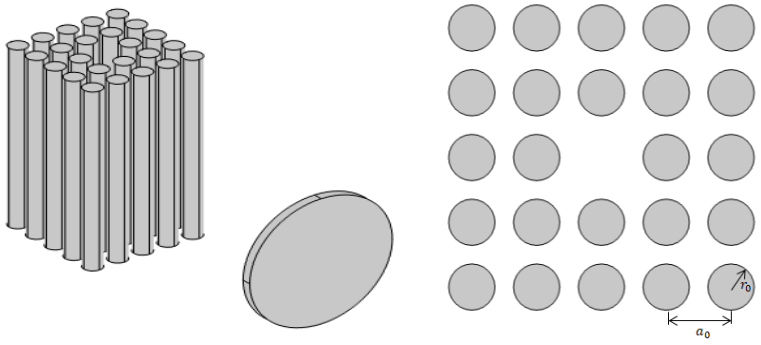

Fig. 1: Model of regular square lattice in COMSOL Multiphysics 6.0

Table 1. Material properties [7]

-	Piezoelectric	PMMA
Density ($\mathbf{kg/m^3}$)	1780	1190
Young's modulus (MPa)	3.8	3
Poisson's ratio	0.3	0.327
Sound velocity ($\mathbf{m/s}$)	-	2694
Relative permittivity	9.3	-

Various lattices considered in this research are shown in Figure 2. In this figure, non-square lattices include circular, rhombus-shaped, and rectangular lattices. Combined lattices are also presented, such as square-rhombic, square-rectangular, and rhombus-rectangular lattices. Also, changing the position of the defect and increasing the number of defects is considered, as shown in Figure 3.

The method of selecting the defect position in the square lattice crystals in cases (7) and (12) was random.

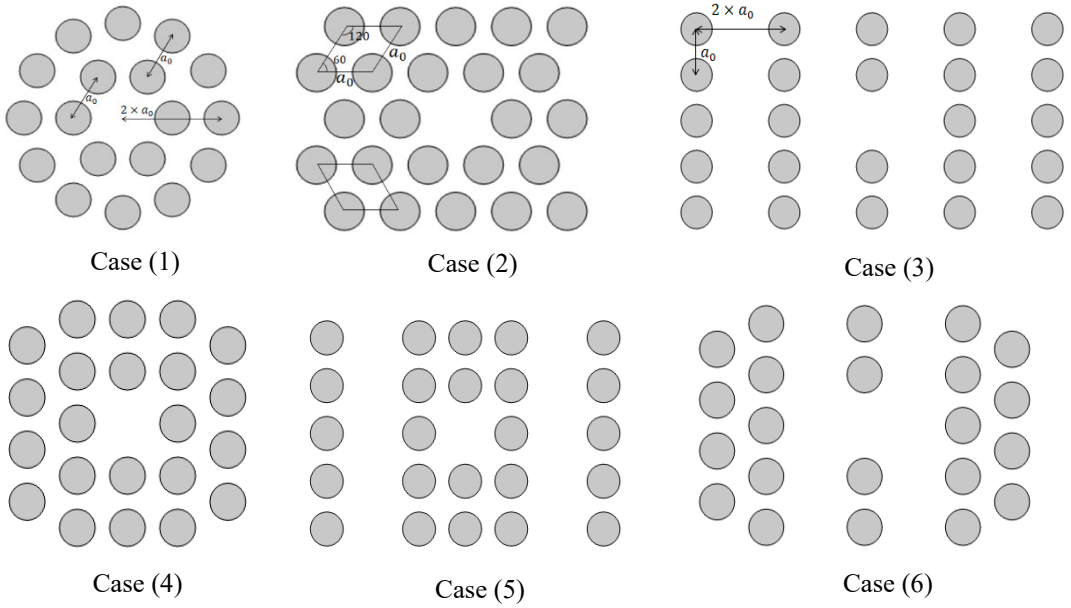

Fig. 2: Lattices: Case (1) circular lattice, Case (2) rhombus lattice, Case (3) rectangular lattice, Case (4) square-rhombic lattice, Case (5) square-rectangular lattice, Case (6) rhombus-rectangular lattice

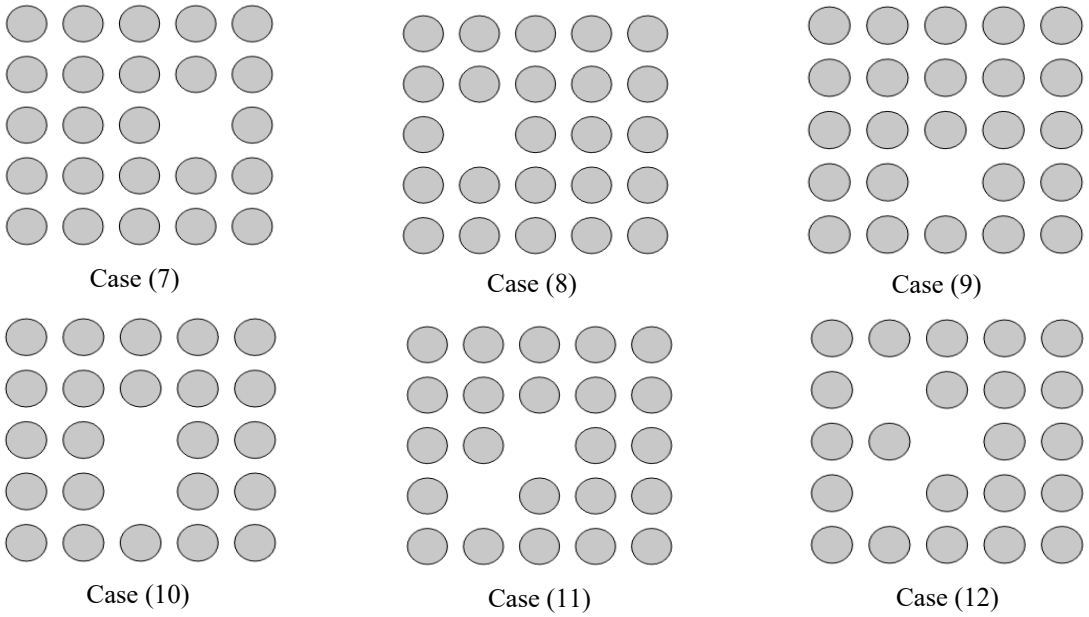

Fig. 3: Position of the defect and the number of defects in a square lattice; Case (7) position of the defect in (a_0,0), Case (8) position of the defect in (-a_0,0), Case (9) position of the defect in (0,- a_0), Case (10) position of defects in (0,0) and (0,- a_0), Case (11) position of defects in (0,0) and (-a_0,- a_0), Case (12) position of defects in (0,0) and (-a_0,- a_0) and (-a_0, a_0)

3. Results and discussions

In this section, the results of SPL and energy harvesting are discussed.

3.1. Sound Pressure Level (SPL)

As mentioned, the current work compares various crystal lattices to identify a suitable model with the maximum SPL to increase acoustic energy harvesting. To validate the results, the velocity diagram obtained from the square lattice in the current research is compared with the work reported by Wu et al. [7]. Figure 4a shows the sound velocity trend obtained from the current study. As illustrated in Figure 4a, the velocity at the center of the defect is observed to be 1 mm/s. In contrast, the velocity in the diagonal space between the crystals at the defect is found to be 5 mm/s. By comparing the results in Figure 4b, it can be observed that they exhibit slight differences from one another. Furthermore, the acoustic resonance frequency is calculated in a regular square lattice equal to 4220.4 Hz, which is very close to the resonance frequency of the referenced work (4.21 kHz) [7].

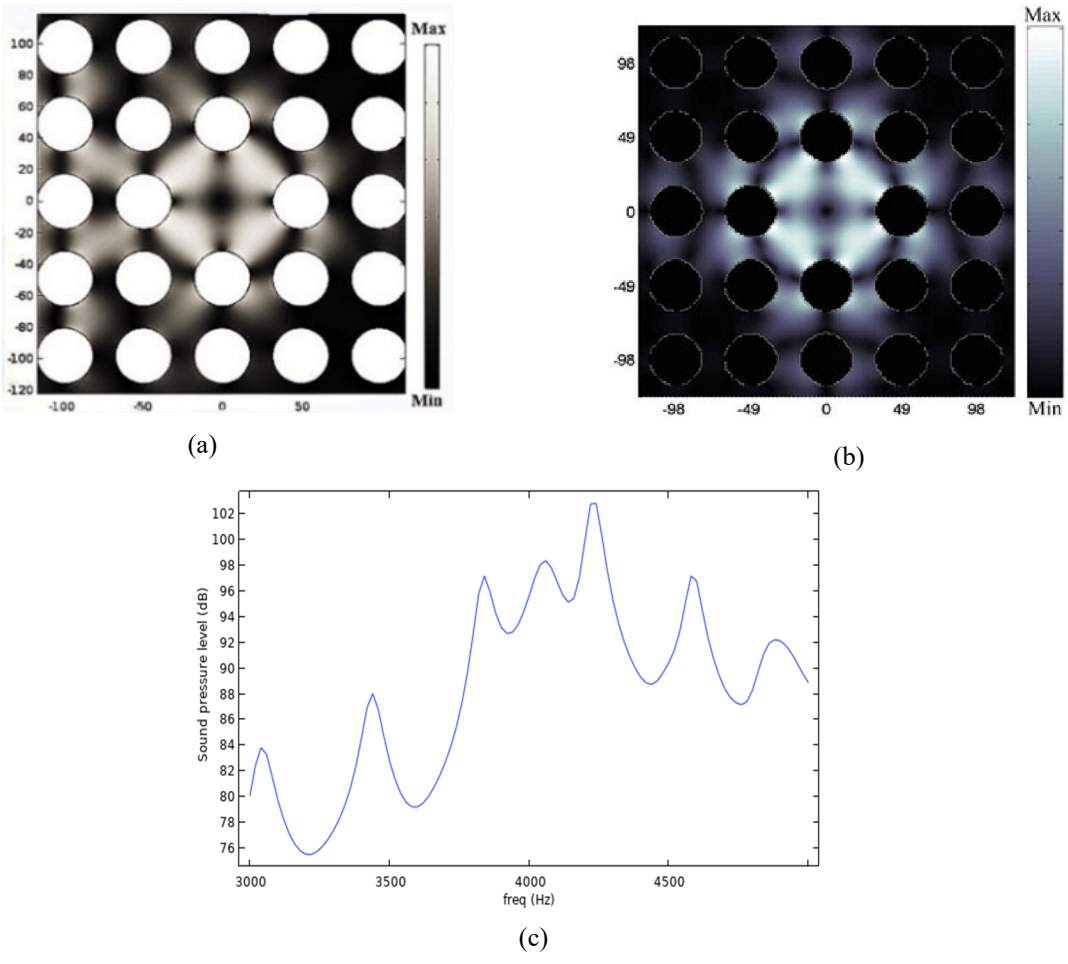

Fig. 4: (a) Sound velocity in the square lattice in the present work, (b) Sound velocity in the square lattice in the referenced work [7], (c) SPL (dB) value according to the frequency (Hz) (the acoustic resonance frequency is 4220.4 Hz)

Figure 5 shows the SPL value as a function of frequency in six different lattices. The wave equation is presented in the following:

$$(C_{11})^{-1}\frac{\partial^2 \vec{P}}{\partial t^2} = \nabla.\left(\rho^{-1}\nabla\vec{P}\right) \quad (1)$$

where $\vec{P}$ is the sound pressure, ρ is the density of the surrounding fluid, $C_{11} = \rho c_1^2$ is the longitudinal elastic constant, and c_1 is the longitudinal sound velocity. On the other hand, the pressure parameter $\vec{P}(\vec{r},t)$, according to Equation (2), must satisfy Bloch's theory as follows:

$$\vec{P}(\vec{r}\ t) = e^{j(\vec{K},\vec{r}-\omega t)} \sum_G \vec{P}_K(\vec{G}) e^{j\vec{G},\vec{r}} \tag{2}$$

where $\vec{K}$ is the two-dimensional Bloch vector, $\vec{G}$ is the inverse lattice vector, and $\vec{r}$ is the position vector. Expanding the quantities $(C_{11})^{-1}$and ρ^{-1} through the Fourier series and then by the placement of Eq. (2) into Eq. (1), the eigenvector relation is obtained as follows [7]:

$$\sum_{G' \neq G} F_G(\vec{G} - \vec{G}')\left[\Delta(\rho^{-1})(\vec{K} + \vec{G}\,), (\vec{K} + \vec{G}') - \Delta(C_{11}^{-1})\omega^2\right]\vec{P}_K(\vec{G}') + \left[\overline{\rho^{-1}}\left|\vec{K} + \vec{G}\right|^2 - \overline{C_{11}^{-1}}\omega^2\right]\vec{P}_K(\vec{G}') = 0 \tag{3}$$

where ω and $\vec{P}_K(\vec{G})$ are the eigenvalues and eigenvectors. According to the eigenvector relation (Equation (3)), in various lattices of the crystal, the coefficients C_{11} , and ρ^{-1} are different, thus the sound resonance frequency and the SPL experience different values.

As shown in Figure 5, in case (1), the maximum SPL is obtained at the frequency of 4620 Hz with a value of 98.04 dB. In case (2), the maximum SPL occurs at the frequency of 4260 Hz, with a value of 90.58 dB. This case has the lowest value compared to other cases. Additionally, the frequency of 3620 Hz corresponds to an acoustic anti-resonance. In case (3), the local maximum SPL is 103.12 dB, which occurs at the frequency of 3820 Hz. In case (4), the maximum SPL is achieved at the frequency of 4220.4 Hz, corresponding to a value of 103.40 dB. This value is the highest compared to the other cases. Therefore, among the lattices, the rhombus-square lattice provides the optimal conditions to harvest the maximum acoustic energy. In cases (5) and (6), the maximum SPL occurred at 3820 Hz and 3860 Hz and are equal to 100.96 dB and 101.44 dB. In case (6), an acoustic anti-resonance frequency is observed, which occurs at a frequency of 3160 Hz, respectively. Table 2 briefly shows the results of the maximum pressure level at a specific acoustic resonance frequency for cases (1)-(6).

Table 2. Comparison of maximum SPL results at a given acoustic resonance frequency for cases (1)-(6).

Case	The acoustic resonance frequency (Hz)	Maximum SPL (dB)
1	4620	98.04
2	4260	90.58
3	3820	103.12
4	4220	103.40
5	3820	100.96
6	3860	101.44

As a result, by comparing the SPL values, it was found that the rhombus-square lattice is the most suitable crystal lattice, in which the SPL value at a frequency of 4220.4 Hz is equal to 103.40 dB. Therefore, this lattice is used in the following simulation to convert mechanical energy into electrical energy.

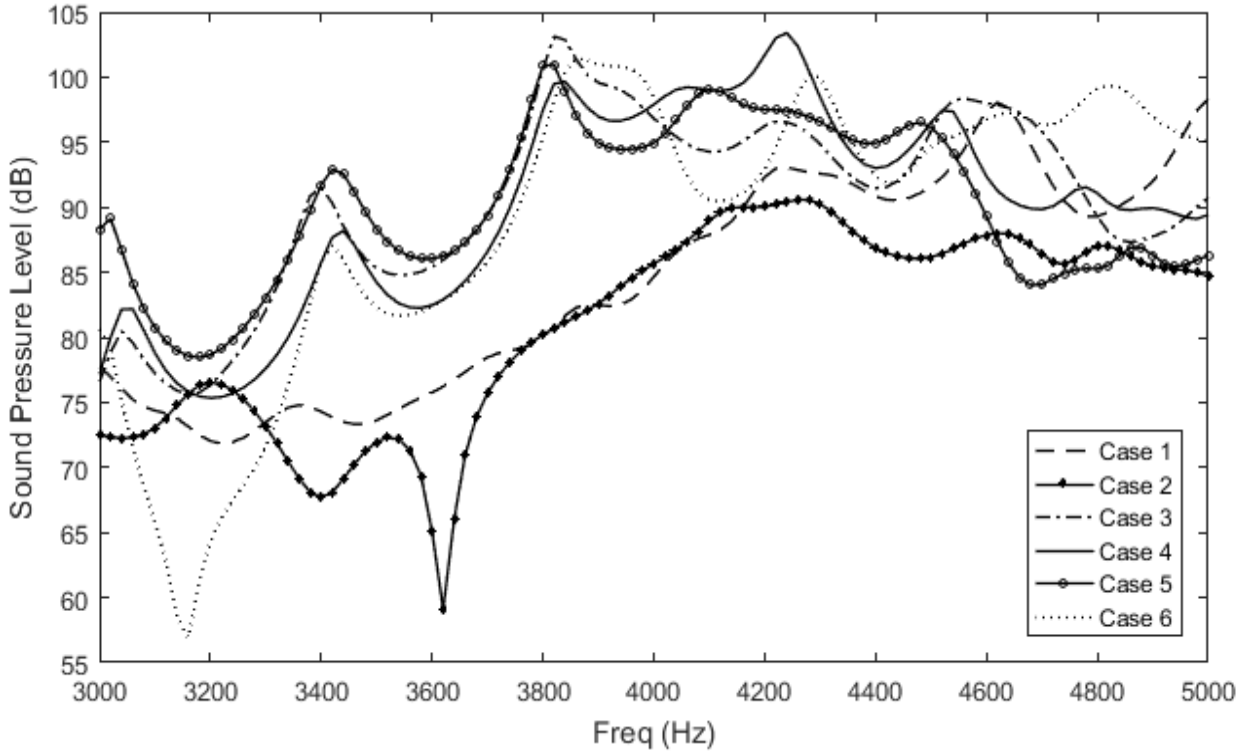

Fig. 5: The SPL (dB) values in terms of the frequency (Hz) in six lattices

Figure 6 shows the SPL values in terms of frequency for cases (7)-(12). As can be seen, changing the position or number of defects in the square crystal lattice results in a negligible difference in the acoustic resonance frequency. This indicates that, in a specific crystal lattice, changing the position of the defect and/or increasing the number of defects does not affect the eigenvector relation (Equation 3). However, these factors have a significant impact on the maximum SPL value. Furthermore, the maximum SPL value is calculated in case (10) to be 105.77 dB at the frequency of 4220 Hz. According to the results of cases (7) and (8), it can be seen that at the same resonance frequency, case (8) (104.76 dB) has a higher SPL value than case (7) (97.13 dB), which confirms the results of Wu et al. [16]. This is because, in case (8), the number of arranged crystal rows after the defect is two, while in case (7), it is one. The results of the maximum SPL at a given acoustic resonance frequency for cases (7)-(12) are summarized in Table 3.

Table 3. Comparison of maximum SPL results at a given acoustic resonance frequency for cases (7)-(12).

Case	The acoustic resonance frequency (Hz)	Maximum SPL (dB)
7	4220	97.13
8	3820	104.76
9	4220	99.09
10	4220	105.77
11	3820	103.08
12	3800	102.74

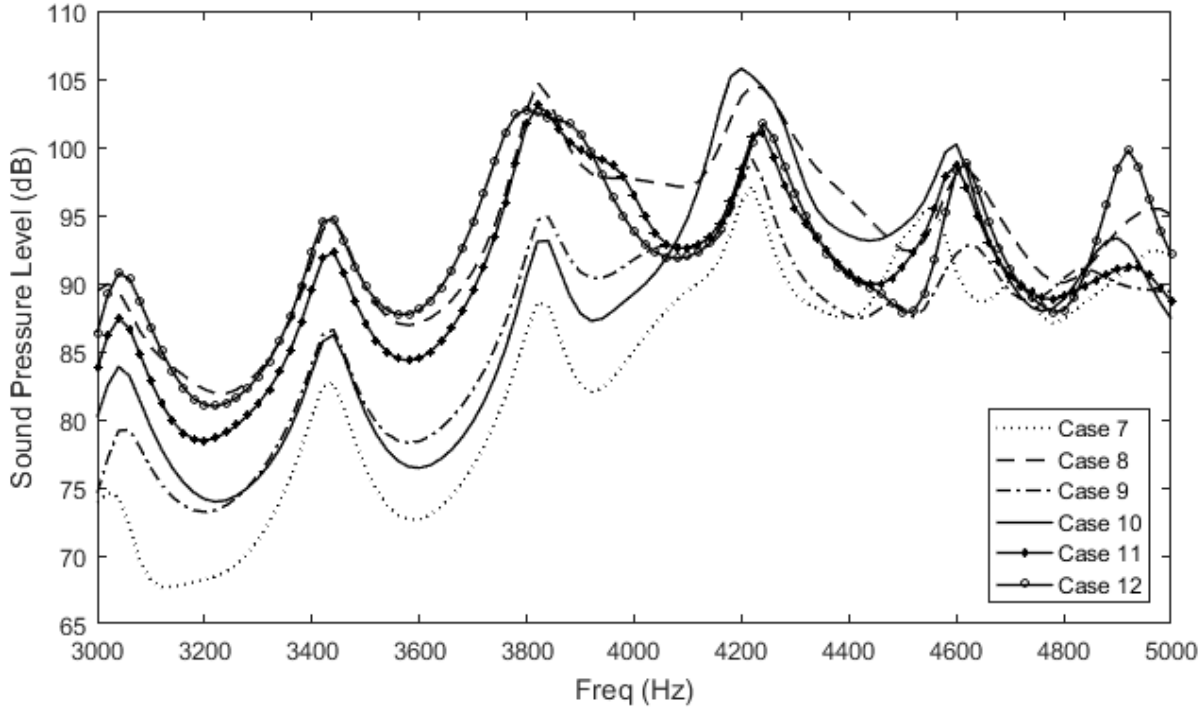

Fig. 6: The SPL (dB) values according to the frequency (Hz) *in six cases*

3.2 Energy harvesting

The maximum SPL value at the defect position in case (4) occurs at a frequency of 4220.4 Hz, corresponding to a value of 103.40 dB. To harvest the maximum energy, the dimensions of the piezoelectric beam are chosen so that the natural frequencies of the beam are close to the acoustic resonance frequency of 4220.4 Hz. Therefore, a PVDF cantilever patch is used with dimensions of $63\times16\times0.028(mm^3)$, which is protected on both sides by two polyester layers with thicknesses of 53 μm and 123 μm. Additionally, the piezoelectric is installed in a position where the largest pressure difference is on both sides.

In Figure 7, the sound velocity between crystals is demonstrated. According to Equation (4), the pressure difference is related to the sound velocity.

$$ev = -\int \frac{1}{\rho_\circ} \nabla p \, dt \tag{4}$$

where v is velocity, $\rho_\circ$ is the fluid density, and p is the sound pressure .In addition, the output voltage from the resistive load R is equal to

$$V = \frac{j\omega \frac{2c_p d_{31} t_0}{\varepsilon}}{j\omega\left(\omega^2 k_{31}^2 + \frac{2\zeta\omega}{RC_b}\right) - 2\zeta\omega^3} \frac{A_{in}}{k} \tag{5}$$

where $\frac{c_p d_{31}}{\varepsilon}$ and $k_{31}^2 = \frac{c_p d_{31}^2}{\varepsilon}$ are the piezoelectric coupling coefficients and k ،A_{in} ،ζ and ω are the geometrical constant, excitation acceleration, mechanical damping, and angular frequency, respectively [18]. The piezoelectric capacity and density are 7000 kg/m^3 and 0.43 nF, respectively.

The optimal position for the piezoelectric installation is the specified position with an angle of 45 degrees to the x-axis. The piezoelectric material is simulated in (-10mm, 10mm, 0) coordinates, which is connected to an electric circuit that includes an electrical resistance.

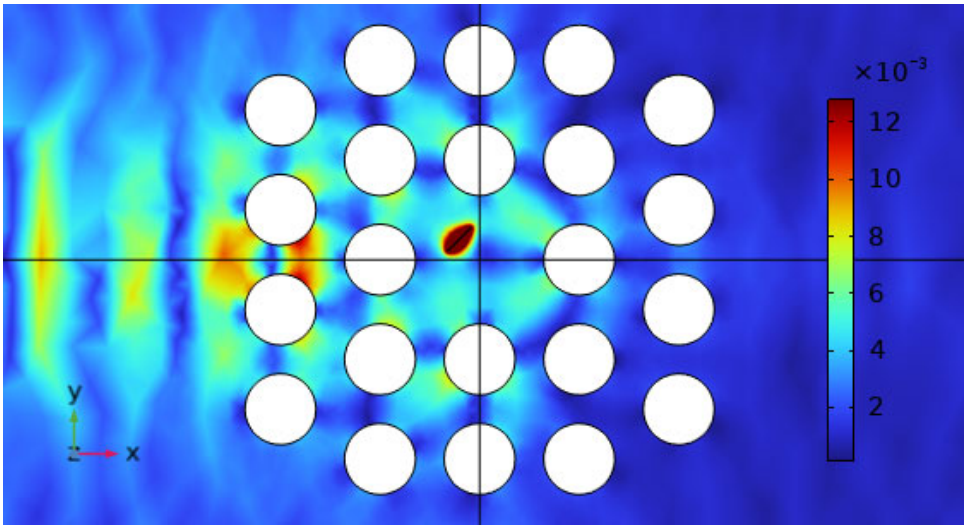

Fig. 7: Velocity contour in the square-rhombic lattice

Figure 8 shows the harvested voltage by piezoelectric according to the frequency in a square-rhombus lattice. In this case, the value of voltage harvested for the optimal resistance is 11.34 mV at the frequency of 4220.4 Hz. Figure 9 shows the voltage and power at different resistances in a square-rhombic lattice. The maximum power value of 4.15 nW is achieved at a resistance of 15 kΩ, which is the optimal resistance. According to Figure 10, the energy can be harvested at five different resonance frequencies by installing three piezoelectric patches in the positions of the three defects (case (12)). This provides better conditions for energy harvesting compared to the single-defect case. As the number of defects increases, the local resonance frequency of the metamaterial increases concomitantly; consequently, according to Equation (5), the number of peaks increases.

In this case, the maximum voltage harvested is 7.98 mV, which is created at the frequency of 3980 Hz.

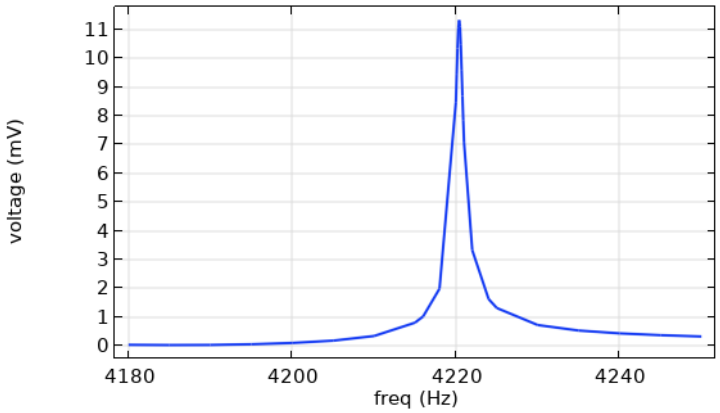

Fig. 8: The voltage (mV) values as a function of the frequency (Hz) in the square-rhombic lattice

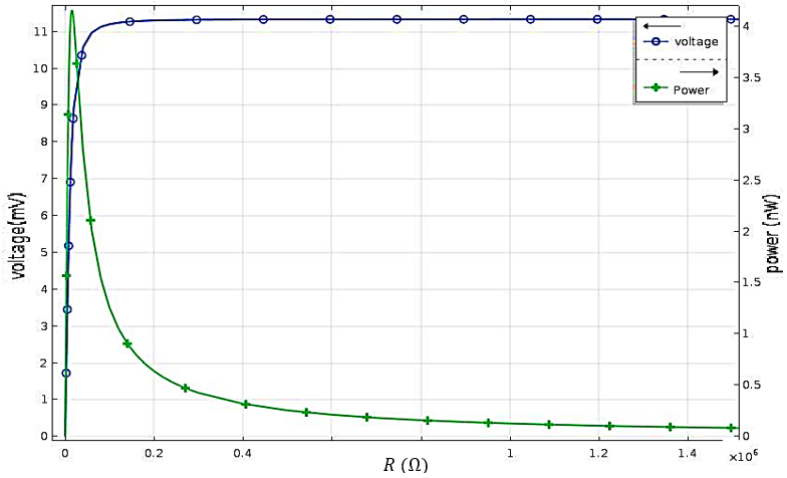

Fig. 9: The voltage (mV) and power (nW) values as a function of electrical resistance (Ω) in the square-rhombic lattice

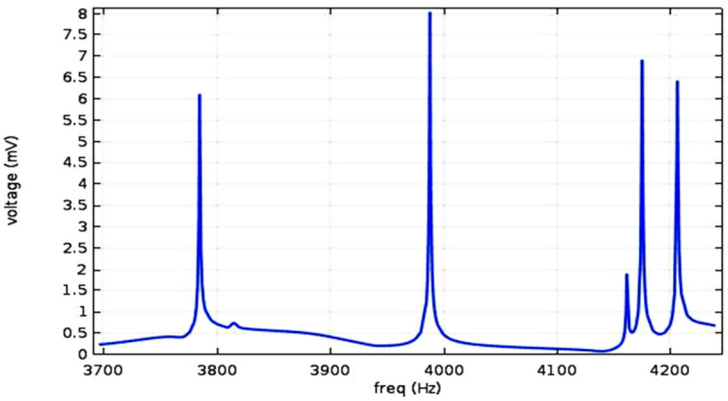

Fig. 10: The voltage (mV) values as a function of frequency (Hz) in case (12)

4. Conclusion

In the present study, an optimal crystal lattice with the maximum SPL value was identified using a variety of lattices, including circular, rhombus-shaped, rectangular, square-rhombic, square-rectangular, and rhombus-rectangular lattices. Furthermore, the impact of modifying the position of the defect and increasing the number of defects on the SPL value in the square lattice of crystals was examined. The results indicated that the square-rhombic lattice exhibited the highest SPL value in non-square lattices. The SPL value obtained in the square-rhombic lattice was equal to 103.40 dB at a frequency of 4240 Hz. The installation of the piezoelectric in the optimal position and utilization of the optimal resistance of 15 kΩ resulted in a harvested voltage and power of 11.34 mV and 4.15 nW, respectively. Additionally, by changing the position of the defect and increasing the number of defects, it was observed that the highest SPL value was achieved in case (10). In this case, the SPL value obtained at the center of the defect was equal to 105.24 dB at a frequency of 4200 Hz. Furthermore, installing three piezoelectric patches in the locations corresponding to the three defects introduced in case (12) demonstrated the potential for energy harvesting at five distinct resonance frequencies. Compared to the single-defect case, the harvesting of higher power in case (12) was observed. As the number of defects increases, the local resonance frequency of the metamaterial rises concomitantly. Consequently, the number of peaks increases. In case (12), the maximum harvested voltage was determined to be 7.98 mV, which was generated at a frequency of 3980 Hz.

References

[1] A. Yang, P. Li, Y. Wen, C. Lu, X. Peng, J. Zhang , W. He, Enhanced acoustic energy harvesting using coupled resonance structure of sonic crystal and helmholtz resonator, Applied Physics Express, 6 (2013).

[2] A. Yang, P. Li, Y. Wen, C. Lu, X. Peng, J. Zhang, W. He, Enhanced acoustic wave localization effect using coupled sonic crystal resonators, Applied Physics Letters, 104 (2014).

[3] A. Yang, C. Lu, F. Wu, L. zhu, M. Pei, P. Liu, M. Li, X. Dai, Extremely-huge wave localization in coupled multilayer heterogeneous phononic crystal resonators, Applied Physics Express, 12 (2018).

[4] T. Jiang, Q. He, Z. Peng, Enhanced directional acoustic sensing with phononic crystal cavity resonance, Applied Physics Letters, 112 (2018).

[5] A. H. Aly, A. Nagaty, Z. Khalifa, A. Mehaney, The significance of temperature dependence on the piezoelectric energy harvesting by using a phononic crystal, Journal of Applied Physics, 123 (2018).

[6] S. Sharifi-Moghaddam, R. Tikani, S. Ziaei-Rad, Energy harvesting from nonlinear vibrations of an L-shaped beam using piezoelectric patches, Journal of the Brazilian Society of Mechanical Sciences and Engineering, 43 (2021) 1-15.

[7] L.-Y. Wu, L.-W. chen, I.-L. Chang, C.-C. Wang, Acoustic energy harvesting using sonic crystals, Advances in Energy Harvesting Methods, (2013) 295-319.

[8] H. Lv, X. Tian, M.Y. Wang, D. Li, Vibration energy harvesting using a phononic crystal with point defect states, Applied Physics Letters, 102 (2013).

[9] A. MacGillivray, R. Racca, Sound pressure and particle velocity measurements from marine pile driving at Eagle Harbor maintenance facility, in, JASCO Research Ltd, Bainbridge Island WA 2005.

[10] M. Yuan, Z. Cao, J. Luo, X. Chou, Recent developments of acoustic energy harvesting: A review, Micromachines, 10.

[11] D. Jang, J. Jeon, S.K. Chung, Acoustic bubble-powered miniature rotor for wireless energy harvesting in a liquid medium, Sensors and Actuators A: Physical, 276 (2018) 296-303.

[12] M.R. Torabi, A. Loghmani, Acoustical simulation, design and experimental investigation of a classroom: A case study, Journal of Theoretical and Applied Vibration and Acoustics 9(2023) 1-20.

[13] H. Samadiyeh, R. Khajavi, MPI- and CUDA- implementations of modal finite difference method for P-SV wave propagation modeling, Journal of Theoretical and Applied Vibration and Acoustics 2(2016) 185-202.

[14] H. Moriyama, H. Tsuchiya, H.T. Uchida, Effect of acoustic radiation from circular plate installed with piezoelectric element on electricity generation performance, Applied Acoustics, 186 (2022).

[15] L.Y. Wu, L.W. Chen, C.M. Liu, Acoustic energy harvesting using resonant cavity of a sonic crystal, Applied Physics Letters, 95 (2009).s

[16] L.-Y. Wu, L.-W. Chen, C.-M. Liu, Experimental investigation of the acoustic pressure in cavity of a two-dimensional sonic crystal, Physica B: Condensed Matter, 404 (2009) 1766-1770.

[17] M. Carrara, M.R. Cacan, M.J. Leamy, M. Ruzzene, A. Erturk, Dramatic enhancement of structure-borne wave energy harvesting using an elliptical acoustic mirror, Applied Physics Letters, 100 (2012).

[18] S.S. Moghaddam, S. Ziaei-Rad, A. Loghmani, Analysis of hyperbolic crystals with non-square lattice for improving acoustic energy harvesting, Smart Materials and Structures, 24 (2024).